Open Peer Review on Qeios

Synthesis, Characterization and Ameliorative Effect of Iron Oxide Nanoparticles on Saline-Stressed Zea Mays

Callistus Izunna Iheme[1], Peace Mmachukwu John[1], Gift Charleswalter[1], Evangelina Ozoemena Ohaeri[1], Elias Emeka Elemike[2], Nsofor Winifred[1], Chidi Uzoma Igwe[1]

1 Federal University of Technology, Owerri

2 Federal University of Petroleum Resources

Funding: No specific funding was received for this work.

Potential competing interests: No potential competing interests to declare.

Abstract

High soil salinity induces osmotic and ionic stress that threaten crop production worldwide and affect food security. Iron oxide nanoparticles were synthesized using an aqueous leaf extract of *Diodella sarmentosa*, and the results of the characterization using FTIR, XRD, EDX, TEM, UV-vis, and SEM revealed the presence of polydisperse spherical iron oxide nanoparticles (FeONPs) with a maximum light absorption wavelength of 380 nm, and a size ranging from 2.22 to 27.83 nm. Foliar application of FeONPs on the salinized *Zea mays* significantly ($p<0.05$) improved the plant's photosynthetic pigments (total chlorophyl (175.71%), chlorophyll a (256.34%), chlorophyll b (77.01%), carotenoid (39.36%), root length (9.87%), and antioxidant enzyme activities. From the findings, it can be deduced that FeONPs can improve the growth and development of saline-stressed *Zea mays* by lessening the negative effects that salt has on the plant.

Callistus I. Iheme[1,2], **Peace M. John**[2], **Gift I. Charleswalter**[2], **Evangelina O. Ohaeri**[3], **Elias E. Emeka**[4], **Chioma Y. Ezirim**[2], **Winifred N. Nsofor**[2], and **Chidi U. Igwe**[1,2]

[1] *Department of Forensic Science, Federal University of Technology (FUTO), Owerri, Nigeria.*

[2] *Department of Biochemistry, FUTO*

[3] *Department of Science Laboratory Technology, FUTO*

[4] *Department of Chemistry, Federal University of Petroleum Resources, Effuru, Nigeria.*

Keywords: iron oxide nanoparticles, soil salinity, maize plant, chlorophyll, antioxidant enzymes.

1. Introduction

The United Nations (2019) projected that there will be 9.7 billion people on Earth in 2050, up from 7.4 billion in 2017. This

population increase has drawn a lot of attention for its potential impact on global food demand. According to estimates from the Food and Agriculture Organization (FAO), there is a need to produce 60% more food by 2050 in order to feed the 9.3 billion people that inhabit the earth. Unfortunately, more than a quarter of the world's arable land is almost completely impacted by soil stress from salt. Around 62 million hectares, or 20% of all arable land, are believed to be affected by salinity at the moment, and this number is projected to keep rising daily, particularly in dry and semi-arid regions of the world. Plant metabolism and physiology are altered as a result of salt buildup in the soil. These plant-related consequences of soil salinity are linked to the toxicity of Na and Cl ions and the low osmotic potential of soil solutions, which results in a water deficit in plant cells (Ahmad et al., 2019; Etesami and Noori, 2019). Salinity stress severely harms both halophytic and glycophytic plants (Etesami and Beattie, 2018; Komaresofla et al., 2019).

When soil salinity exceeds thresholds for any given crop, crop yield is decreased; sweet potato, wheat, and maize are particularly sensitive, while cotton, barley, and sugar beet are highly tolerant. The ions of Cl, Mg, SO_4, or HCO_3 are additional causes of salt toxicity in addition to Na^+ (Zörb et al., 2019). Early in a plant's life, salt stress can severely limit growth, which will negatively impact yield and lower the quality and amount of plant products produced. Despite its subtle impacts, salt can reduce agricultural yields. A crop's capacity to draw water and nutrients from saline soils and prevent an excessive buildup of salt ions in its tissues determines both its sensitivity to salt and its tolerance to it (Kaleem et al., 2018; Khan et al., 2017; Ahmad et al., 2017).

One possible tactic to combat the issue of declining global food production is the breeding of salt-tolerant plants and the development of salt-resistant agricultural variants. However, using inter-specific or inter-generic hybridization to increase crop plants' stress tolerance has proven to be less effective with conventional breeding techniques (Fita et al., 2015). Lately, a number of studies (Etesami and Glick, 2020; Etesami and Jeong, 2018; Liang et al., 2018) have concentrated on novel approaches to address salinity in order to reduce its detrimental effects on plants.

Nanotechnology has recently caught the attention of research experts from numerous disciplines of science and plays an important role in medicine, agriculture, industry, the environment, energy, and electronics (Alvarez-Chimal & Angel Arenas-Alatorre, 2023). Because of their unique features, nanoparticles (NPs) have multiple novel applications in several disciplines of science. In agriculture, nanoparticles increase crop productivity by improving plant nutrition concentration and water consumption efficiency, as well as crop protection against pests and diseases using molecular tools and procedures, and environmental protection by increasing plant tolerance to biotic and abiotic stress while reducing environmental pollution to the barest possible minimum (Singh et al., 2023).

A variety of parameters, including concentration, size, treatment application method, plant absorption, characteristics, reactivity, and translocation into different tissues, influence how distinct metabolic activities of nanoparticles (NPs) affect plants (Mattiello et al., 2015; Paramo et al., 2020). While there are intriguing uses for NPs in agriculture, it is well known that there are still many unanswered questions about the harm that these substances can cause to the environment, especially to plants and other living things (Tripathi et al., 2017a). The discovery of NPs' extensive applications in plant science and agriculture is still largely disputed (Nair et al., 2010).

Nanoparticles range in sizes between 1 and 100 nm, and they exist as organic, inorganic, and carbon-based nanoparticles (Mauricio et al., 2018). Methodologies, such as the physical method, chemical method, and green method, have been employed over the years in synthesizing nanoparticles. The physical methods are quite effective but require expensive apparatus and setup. Chemical methods involve the use of chemical agents. It causes a sizable quantity of chemical waste to be produced as a byproduct, contaminating the environment in the process. The green methods require organic precursors such as plant extracts, bacteria, and fungi. It's the most considered in recent times for the biosynthesis of various metal nanoparticles (Šutka et al., 2020). The process is known as green synthesis, and it is both cost-effective and beneficial to the environment (Iqbal et al., 2020).

One of the essential micronutrients for plants is iron. It is significant because it plays a key role in metabolic processes like respiration, photosynthesis, and DNA synthesis (Rout &Sahoo, 2015). Hence, an obstruction in iron uptake is a limiting factor in plant biomass production. Nanoparticle-based iron fertilizer can act as a bioavailable iron reservoir for plants, as they seem to have immense potential for success in the agricultural sector due to their low levels of toxicity and affordability. Over time, scientists have examined several forms of iron nanoparticles to evaluate their beneficial impact on plant growth and metabolism (Maria et al., 2022). The application of iron oxide nanoparticles to soil was found to considerably improve the morphological qualities of plants, such as the number of leaves, the percentage of sprouting, the biomass of the plant, the biomass of the shoots and roots, the characteristics of the roots, and the duration of the first leaf appearance phase (Haydar et al., 2022). However, this study looked at the biochemical effects of applying Fe nanoparticles to the leaves of saline-stressed *Zea mays*.

Using extracts from plants' leaves, seeds, roots, stems, fruits, and bark, different types of Fe-NPs have been synthesized to carry out research work by researchers (Šutka et al., 2020; Kumar 2021). Iron nanoparticles have been employed in medicine, industry, agriculture, and laboratories. In crop production, iron nanoparticles (Fe-NPs) enhance plant growth and development by helping to increase germination and growth response (Etesami et al., 2021). In this study, the ameliorative effects of the biosynthesized FeONPs on the saline-stressed *Zea mays* were assessed.

2. Materials & Methods

2.1. Sample Collection and preparation

A taxonomist from the Department of Forestry and Wildlife at the Federal University of Technology Owerri identified the fresh leaves of *Diodella sarmentosa (SW)* that had been obtained from the university's premises. Next, the leaves were carefully removed from the stems and thoroughly rinsed under running tap water. The water was then allowed to completely drain from the freshly cleaned leaves.

A 200 mL aqueous solution containing five grams of the pulverized dried leaves was heated to 100°C for 1 hour. The solution was heated, filtered, and evaporated until it was completely dry. The crude extract was then removed and stored at -4 °C for additional research.

2.2. FeONPs Synthesis

Diodella sarmentosa crude extract (0.1 g) was reconstituted in 200 mL of deionized water to provide a clear yellowish solution, which was subsequently used to produce FeONPs. The leaf extract filtrate was then mixed with a 0.02 M (1.08 g) solution of $FeCl_3.6H_2O$ to form a yellow solution. Iron oxide nanoparticles (FeONPs) were formed when the solution was heated to 80 °C for 30 minutes while being constantly stirred. This caused the solution's hue to change from yellow to black.

For ten minutes, it was centrifuged at 4000 rpm. The resulting colloidal particles were then dried and examined further (see Fig. 1 for a schematic representation of the experimental set-up).

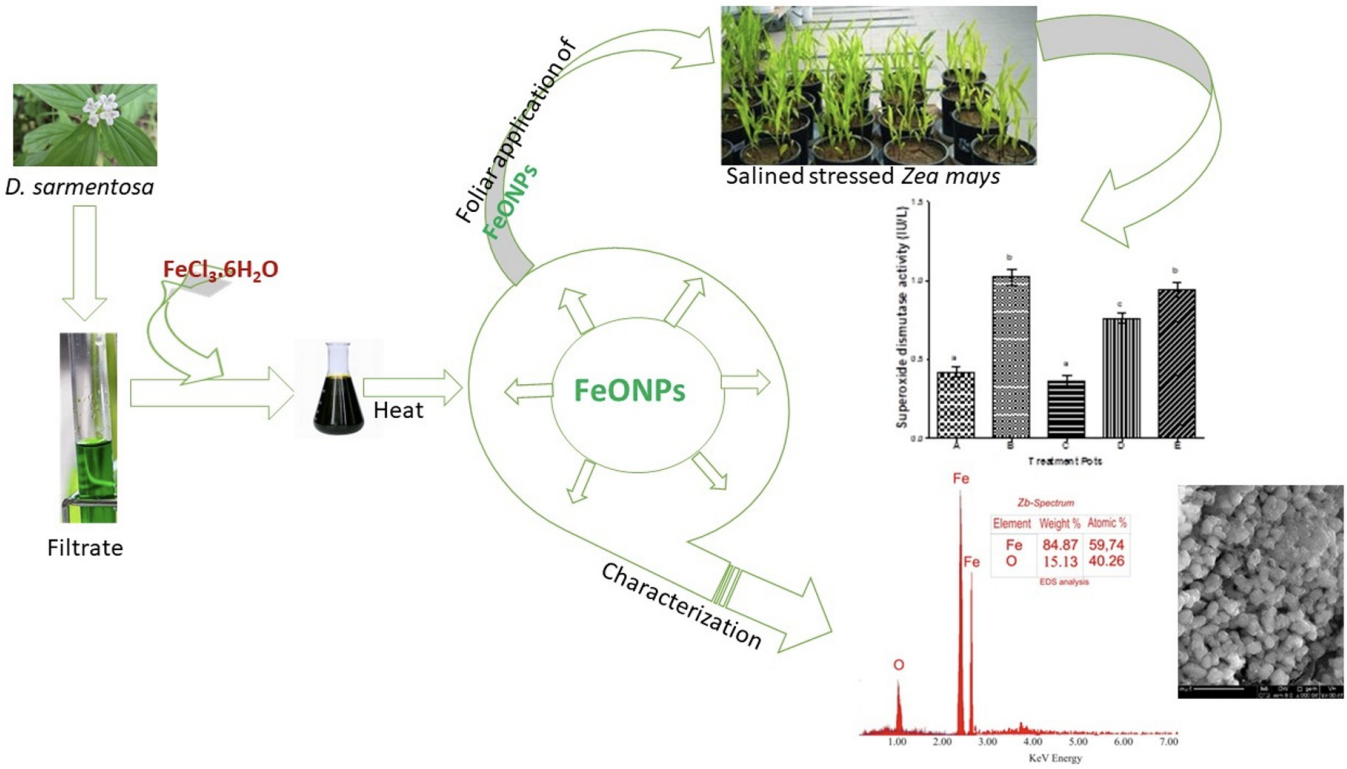

Figure 1. The experimental set-up

2.3. Instrumental analysis of the nanoparticles

UV-vis spectroscopy was performed using a Genesys UV-VIS Spectrophotometer, model Prove 30, with serial number 2130315791 and software version ISW 1.5.1. The wavelength range in which the absorption spectra were recorded was 200 nm to 900 nm.

The possible phytochemicals that capped the FeO NPs were identified by their functional groups using FTIR equipment. During the experiments, the FTIR spectra were collected in the frequency range of 800-4000 cm^{-1}.

A wide-angle x-ray diffraction pattern for iron oxide nanoparticles was obtained using a Rigaku D/Max-IIC X-ray

diffractometer (Rigaku Int. Corp., Tokyo, Japan) fitted with a 2θ compensating slit, CuKα radiation (1.54 Å) at 40 kV, 40 mA passing through Ni filter with a wavelength of 0.154 nm at 20 mA and 35 kV. Over a 2θ range of 20–90, data was collected continuously in scan mode with a step size of 0.01 and a step time of 1 s. PC-APD diffraction software was used to analyze the data. The potential size was estimated using the Scherrer equation $\beta=k\lambda/L\cos\theta$, where k is the shape factor (which ranges from 0.62 to 2.08, measured at intervals of 0.59), L is the nanocrystalline material's size, θ is the diffraction angle, λ is the wavelength, and β is the peak width at half maximum (FWHM), which was calculated from the diffraction pattern at a 2θ angle of 20 degrees.

An EDX device was used to assess the reduced iron oxide nanoparticles' energy content and purity. The morphological properties of the produced FeONPs were investigated using a SEM (JEOL JSM-6380 LV, operating at 20 Kv) in order to determine the microstructure of the nanoparticles. After the sample was evenly distributed onto a SEM holder, its conductivity was increased by covering it with gold (Au). In addition, a Tecnai G2 Stwin model running at 200 kV was utilized as a High-Resolution TEM to measure the nanoparticles' particle diameter. After being ground into a powder, the sample was placed on carbon-coated copper grids, sonicated, and inspected under a microscope.

2.4. Seed and Soil Preparation

Viable *Zea mays* grains were sterilized with a sodium hypochlorite solution (4%) for a minute, then rinsed twice with distilled water. The sodium hypochlorite acted as a disinfectant to ensure healthy seeds. The soil was collected from a non-contaminated area on the premises of FUTO. The soil sample was sieved to remove gravel and debris using a 2mm mesh, and an equal quantity of the homogenized soil sample was placed in five different plastic pots labeled A, B, C, D, and E.

2.5. Pot Experiment

In each pot (A, B, C, D, and E) containing an equal quantity (4.5kg) of homogenized loamy soil, five grains of *Zea mays* were planted.

Each pot was irrigated with portable water for the first fifteen (15) days. Following the germination of the grains in each pot, pots B, D, and E were irrigated with 200 ml of a 300 mM solution of sodium chloride (NaCl) for the subsequent ten (10) days. Pots A and C received portable water throughout the experiment. After the ten days of treatment period, the seedlings in pots B, D, and E were irrigated in the subsequent five (5) days with portable water to enable system adjustment.

Afterwards, each seedling in pots C and D received daily 5 ml foliar applications of the FeONP solution (1: 10 g/ml of the FeONP to distilled water) for 10 days. Similarly, each seedling in pot E also received a 5 ml foliar application of a bulk solution of $FeCl_3.6H_2O$ (1:10 (g/ml) bulk $FeCl_3.6H_2O$ solution to distilled water) for 10 days. After the ten days of treatment, the samples were allowed five (5) additional days before uprooting.

During foliar applications, the pot surfaces were covered with plastic film to prevent contact with the soil. After 45 days,

the seedlings in each pot were uprooted and washed under running tap water. The samples were allowed to drain off water, measured, homogenized, and stored in sample bottles for further analysis.

2.6. Macroscopic Examination

Each day from the germination of the seedlings to the 45 days of the experiment, the height of the plumule (seedling) in each pot was measured in mm. The roots (radicals) of each seedling were measured in mm at the end of the pot experiment. Other observations made were the weight of the plumule (seedling)—fresh and dry weight—color, as well as the appearance of the leaf area.

2.7. Assessment of Antioxidant Enzyme Activity

To assess the antioxidant enzymes' activities, the enzymes were extracted using the Mukherjee (Mukherjee, 1983) method by adding 0.5g of the fresh leaf into 10 ml of phosphate buffer (KH_2PO_4/K_2HPO_4) and centrifugation at 1500 rpm at 4 °C for ten minutes. The supernatant was preserved in the laboratory at a temperature of 4°C to further analyze CAT and SOD activities.

In the assay, a mixture containing 0.1 ml of the sample, 1.1ml ml of 50 mM phosphate buffer (pH = 7.4), 0.4 ml of 1% V/V Tween 80, 0.075 ml of 20 mM L-Methionine, 1.4 ml, and 0.075 ml of 10 mM hydroxylamine was prepared and placed in an incubator for 5 minutes at 30 °C. After this, a small quantity of riboflavin was added (80µl of 50µM riboflavin), followed by exposure of the tubes to incandescent light (200 watts lamp) for 10 minutes. Thereafter, 0.5 ml of 1% sulphanilamide and 0.5 ml of 0.1% NED were added, and a color formation was observed at a maximum absorbance of 543nm. One unit of enzyme activity was defined as the amount of SOD needed to stop 50% of the nitrate from forming under the test conditions.

The measurement of catalase enzyme (CAT) activity was done using the method of Aebi (1984). The method is based on the principle of inducing the decomposition of hydrogen peroxide in the presence of the CAT enzyme and thereafter measuring the subsequent reduction in absorbance of the test sample. The resulting rate is reported by obtaining the value of the decrease in absorbance at 240nm in 3 minutes.

The assay was performed in 1.5 ml of a reaction mixture containing 1.4 ml of 13.2 mM H_2O_2 in 50 mM phosphate buffer (pH = 7.0) and 0.1 ml of plant tissue homogenate. The rate of decomposition of H_2O_2 was measured in a spectrophotometer at 240nm at 1-minute intervals for 3 minutes. The enzymatic activity of the catalase enzyme (CAT) was expressed in international units per mL (Zhang et al., 2006).

2.8. Assessment of Chlorophyll a and b

The chlorophyll determination was done according to the method of Mittal et al., (2011). Accordingly, 0.25g of the fresh leaves was pulverized with 5 ml of four-fifths (80%) acetone, then placed in a centrifuge for 10 minutes at 3000 rpm at 4 °C. This was followed by analysis with a UV-visible spectrophotometer to determine the specific concentrations of

chlorophyll a and chlorophyll b.

2.9. Determination of per centage indices

The per centage chlorophyll contents, root and shoot lengths, and enzyme activities were determined in all test pots (B, C, D, and E) with respect to the normal control pot A using the formula:

$$\% \text{ index} = \frac{T - C}{C} \times 100$$

where T= test value, C = control value

2.10. Statistical Analysis

A two-way ANOVA was used to plot the mean ± standard deviation of the values that were collected in triplicate. The values were considered statistically significant at $P \leq 0.05$.

3. Results

3.1. FTIR spectroscopic analysis

For the purpose of identifying and characterizing the organic compounds that capped FeONPs, the fourier-transform infrared (FTIR) approach was adopted in identifying the distinctive functional groups. The results of the FTIR spectra provided precise designations for the detected absorbance peaks (supplementary attachment 1). The vibration at about 873.2334 cm^{-1} was identified as being caused by C-Cl stretching in a chloro compound. The peak at about 1430.786cm^{-1} is an indication of ethene compound of CH anti-symmetric stretching. The medium band approximating 1611.548 cm^{-1} and 3426.101 cm^{-1} absorbance signals corresponded to N-H stretching in 1^0 amine and 2^0 amine compounds, respectively. In a cyclic ester, CO symmetric stretch was indicated by an absorbance signal at 1850.270cm^{-1}. The signal, which was about 2062.780 cm^{-1}, represented COO stretching in a carboxylic acid, whereas the absorbances observed around 2445.944cm^{-1} and 2521.164cm^{-1} were ascribed to nitrile compounds with CN anti-symmetric vibrations respectively. Some weak bands around 2738.010cm^{-1} and 2840.874cm^{-1} are ascribed to methylene compounds with CH stretching vibration. The wavelength around 1850.270cm^{-1} is ascribed to cyclic ester compounds having C0 stretching vibrations. Vibration signals between 3068.412 cm^{-1} and 3188.777 cm^{-1} were linked OH symmetric stretching in 1^0 alcohol. While the OH symmetric stretching vibration in 3^0 alcohol was found to be associated with the absorbance ranges of 3773.437cm^{-1} to 3924.950cm^{-1}. The composition of the phytochemicals that capped the synthesized FeONPs can be better deciphered from these observed functional groups (supplementary attachment 1).

3.2. Uv-vis

The synthesized FeO nanoparticles' absorption spectra, which were measured in the 200–900 nm range using a UV–visible spectrometer (UV–2130315791 series), are shown in Figure 2. A spectral bandwidth of 1.0 nm and a scan speed of more than 480 nm per minute were used to record the spectra. The plot of the absorbance against wavelength indicated a spectral peak of absorbance of 3.74 at the 380 nm wavelength, indicating this wavelength to be the optimum for FeO nanoparticles. This is contrary to Tharani et al., (2015), who reported the maximum absorption peak of Fe-NPs at 272nm. This variation may be related to the concentration of the phytochemicals involved in the synthesis.

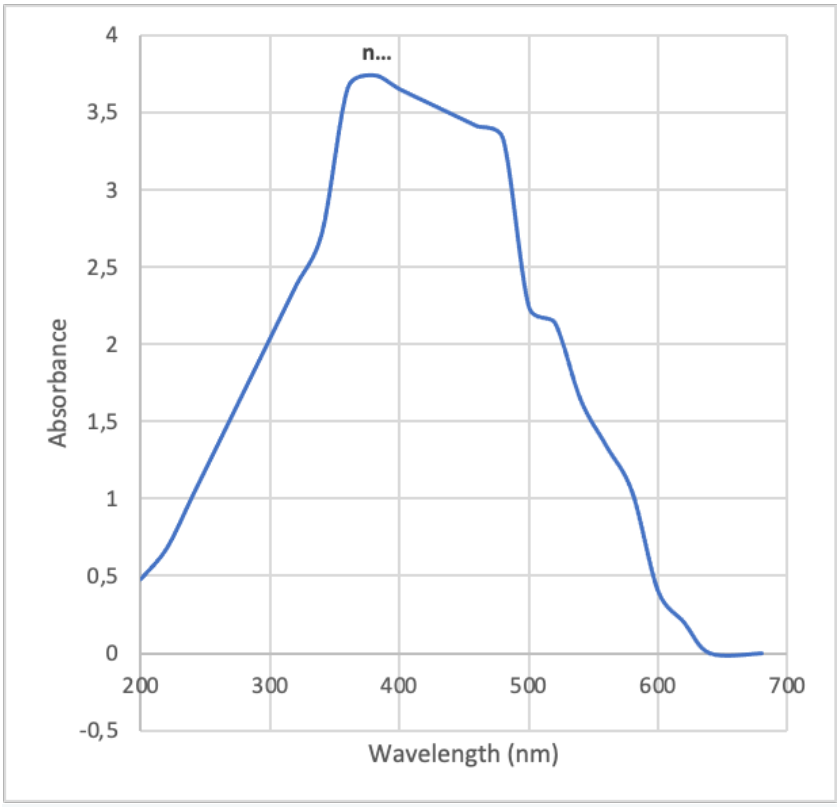

Figure 2. Graph of wavelength against absorbance

3.3. Microscopic studies of the synthesized nanoparticles

The TEM and SEM images of iron oxide nanoparticles are displayed in Figures 3a and 3b. The images graphically represent the topographical, morphological, and size properties of the nanoparticles, providing important information about how their shapes were formed. The TEM image reveals the interior structure and makeup of the FeONPs, which, at 200 nm magnification, display different sizes within a spherical shape. The nanoparticles' average particle diameter varied from 2.22 nm to 27.83 nm.

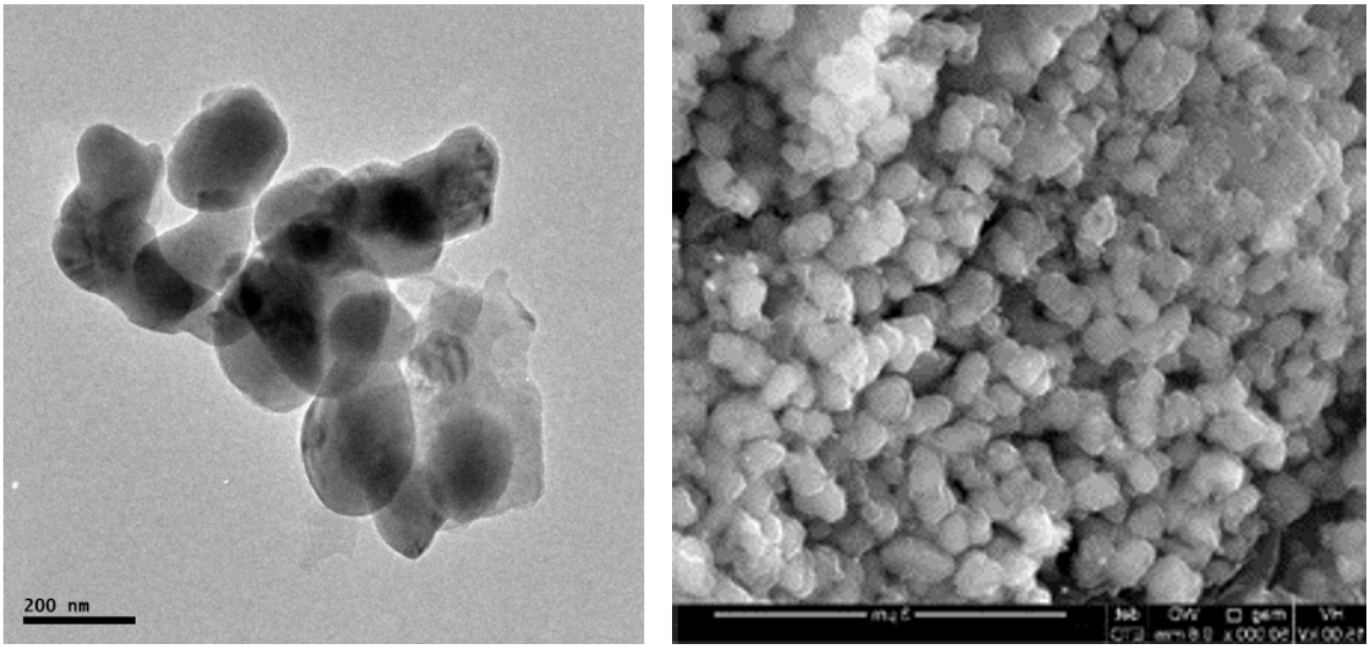

Figure 3. TEM and SEM images of synthesized iron (Fe) oxide nanoparticles

3.4. Energy dispersive X-ray spectroscopy (EDX)

The purity and the energy content of the synthesized FeONPs were determined with EDX. The result of the EDX analysis for FeONPs produced with an aqueous leaf extract of *Diodella sarmentosa* showed that iron constituted 84.87% of the total weight and had the most noticeable energy peak at about 2.5 keV, according to the spectral image. The percentage composition of oxygen was 15.13%, according to the data (Fig. 4).

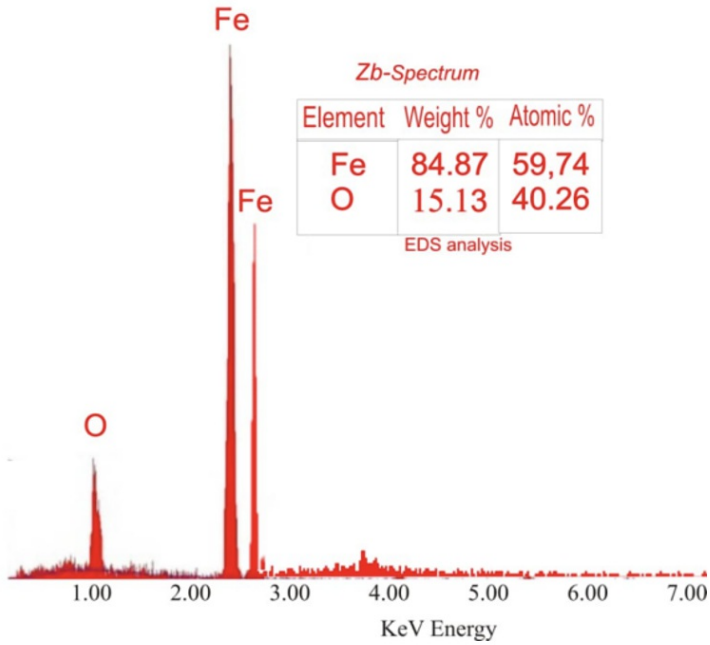

Figure 4. EDX spectral image of synthesized Iron oxide (FeO) nanoparticles

3.5. XRD

Figure 5 displays the X-ray diffractogram of the synthesized iron oxide nanoparticles, where the 2θ values range from 20.52 to 80.30◦. The spectral image revealed that the iron (Fe) nanoparticles have no prominent peak, thus suggesting that the surface structure of the sample is amorphous.

The resulting relative intensity and d value from the diffraction data were compared to the conventional FeO crystallographic data. The average particle diameter size (D), and the average distance between planes of the FeONPs atoms (d-spacing) were determined as 3.03 nm and 3.23 nm respectively (Table 1). This is consistent with the report of Shah et al., (2021) and Achilles *et al;* (2013).

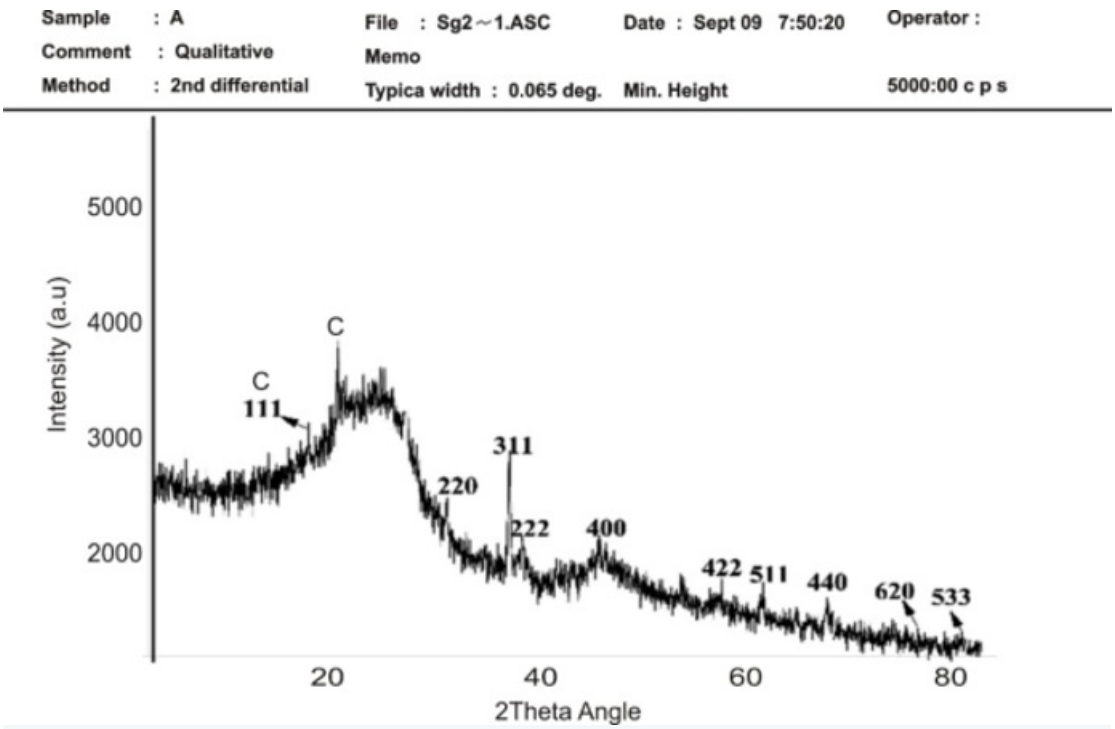

Figure 5. XRD image of synthesized Iron (Fe) nanoparticles

Table 1. XRD Values (D and d) for the synthesized nanoparticle

Peak no.	2theta	FWHM	d-value	Intensity	I/Io	D Values
1	20.52	0.02	2.33	3000	11	7.84
2	24.58	0.03	2.21	3500	14	4.89
3	30.28	0.14	2.22	5000	10	1.03
4	35.30	0.12	2.35	2500	9	1.21
5	38.29	0.12	3.21	3000	9	1.24
6	39.19	0.12	3.22	2000	6	1.22
7	45.20	0.02	3.58	2000	24	6.60
8	52.30	0.13	3.36	2000	10	1.15
9	62.40	0.12	3.26	2000	12	1.35
10	70.10	0.19	4.06	1500	10	0.88
11	75.20	0.02	4.58	1000	24	7.62
12	80.30	0.13	4.36	1000	10	1.35
Average			3.23			3.03

3.6. Macroscopic measurement

An observed decrease in the shoot and root lengths of the salinized plant when compared with the control were recorded. An increase was also observed in the root of the plant treated with FeONPs (supplementary attachment 3) when compared with the control and untreated plants (Tables 2 and 3). This agrees with Farooq et al., (2015), who reported that

when maize plants first experience salt stress, there is an inhibition in shoot growth for maize plants, and salt stress adversely affects seed germination by reducing the soil's potential to move water from high concentration regions to low concentration regions.

Table 2. Weekly Length (cm) of Plumule in each Pot

Weeks	A	B	C	D	E
1	0.60 ± 0.02^{a}	1.50 ± 0.25^{b}	0.80 ± 0.15^{a}	0.70 ± 0.10^{a}	0.60 ± 0.08^{a}
2	6.70 ± 0.11^{a}	13.12 ± 0.58 b	10.72 ± 0.18^{c}	7.70 ± 0.15^{d}	8.60 ± 0.15^{e}
3	17.40 ± 0.65 a	23.12 ± 0.53 b	21.62 ± 0.18^{c}	20.73 ± 0.15^{c}	20.99 ± 0.19^{c}
4	26.80 ± 0.55^{a}	25.02 ± 0.53 b	27.82 ± 0.13 cd	27.03 ± 0.15^{ac}	28.59 ± 0.19^{d}
5	34.10 ± 0.65^{a}	29.12 ± 0.53 b	34.52 ± 0.13^{a}	32.03 ± 0.15^{c}	33.49 ± 0.19 a
6	40.40 ± 0.65^{a}	30.62 ± 0.53^{b}	41.82 ± 0.13^{c}	34.40 ± 0.20^{d}	35.99 ± 0.19^{e}

Table 3. Root Length of Plants in Each Pot (In Cm)

Grains	A	B	C	D	E
1	30.00 ± 0.15^{a}	29.00 ± 0.09 b	30.00 ± 0.13 a	28.00 ± 0.36^{c}	30.00 ± 0.20^{a}
2	27.00 ± 0.05 a	30.02 ± 0.10 b	24.02 ± 0.14^{c}	32.00 ± 0.26 d	30.00 ± 0.17^{b}
3	21.00 ± 0.10 a	20.00 ± 0.09 b	23.00 ± 0.17^{c}	22.00 ± 0.17 d	25.00 ± 0.19^{e}
4	16.98 ± 0.08 a	15.00 ± 0.09 b	18.02 ± 0.20^{c}	21.03 ± 0.12 d	24.99 ± 0.17^{e}
5	17.00 ± 0.05 a	14.98 ± 0.16 b	18.05 ± 0.28 a	20.00 ± 0.20^{c}	16.00 ± 0.95 ab

Values with different superscript letters per row are statistically significant ($p<0.05$).

The root length (Table 3) and average root length per experimental pot (Fig. 6) indicates that salinity stress statistically ($p<0.05$) caused a decline in the average root length of the *Z. mays.* The root lengths were, however, improved on treatment with the FeONPs and the bulk $FeCl_3.6H_2O$ (Supplementary attachment 4). This finding is consistent with the findings of Feng et al. (2022), who suggested that iron (Fe) is an element that promotes plant growth because it can form bigger complexes with different molecules and increase the amount of iron that is available to plant organs.

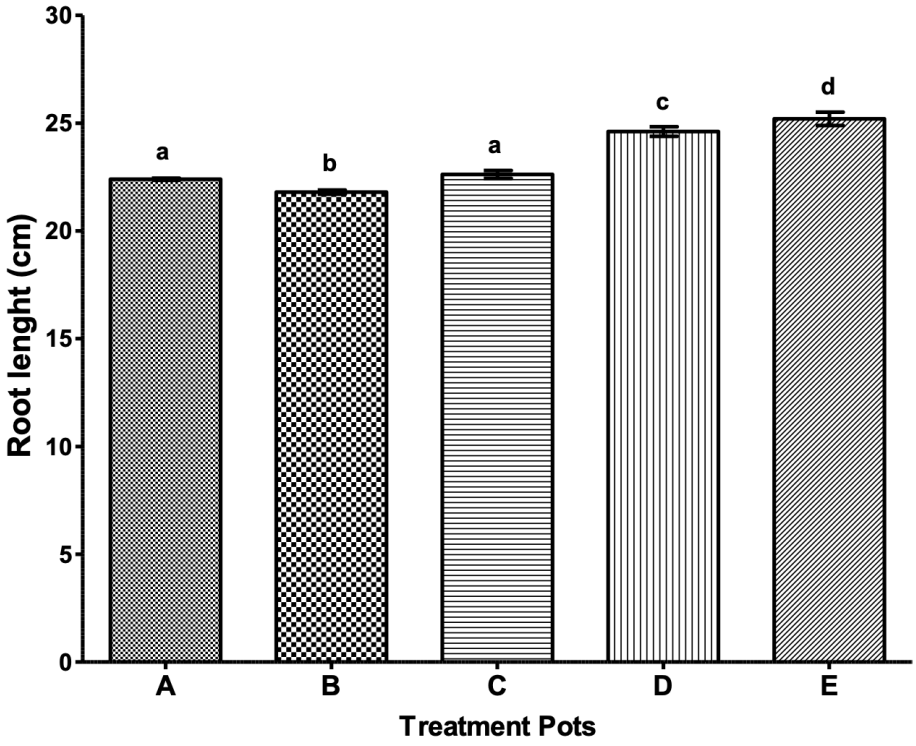

Figure 6. Average root lengths (cm) of the plants in the treatment pots. The figures represent the average ± standard deviation of the triplicate determinations for five grains in each pot. Significant statistical differences are indicated by distinct superscript letters for each row ($p<0.05$).

3.7. FeONPs ameliorative effects on salinized plants

Elevated salt levels in the soil can cause oxidative stress in plants (Isayenkov and Maathius, 2019). As a result, reactive oxygen species (ROS) like hydroxyl radicals ($^{\bullet}OH$), hydrogen peroxide (H_2O_2), and superoxide radicals ($O2^{\bullet-}$) are generated in the affected plants. These ROS can damage plants' DNA, lipids, and proteins, among other biological constituents. To protect themselves from the detrimental effects of ROS and preserve cellular redox balance, plants activate their antioxidant defense mechanisms. These antioxidant enzymes help plants resist salt-induced oxidative damage early in the exposure process. Increasing salt concentrations, however, may overwhelm the activities of these enzymes. In order to keep superoxide radicals from accumulating, superoxide dismutase (SOD) catalyzes their conversion from superoxide radicals ($O_2^{\bullet-}$) into oxygen and H_2O_2. Catalase is able to prevent the formation of hydroxyl radicals and other hydrogen peroxide-derived ROS by breaking down hydrogen peroxide (H_2O_2) into water and oxygen (Haydar et al., 2022).

Another negative impact that plants growing in saline soils experience is osmotic stress, which results in a water shortage. Osmotic stress can interfere with photosynthetic processes, which can negatively impact plant growth and development. When the water potential of the soil in which plants grow is less than that of the soil, the plants absorb water through their roots. Plant water absorption and availability are restricted when there are too many soluble ions in the soil, such as Na+, which lower the water potential of the soil surrounding the root surface (van Zelm et al., 2020). Stomatal closure and disruption of photosynthetic pigments can result from a water deficit (Chaves et al., 2009; Martin-Stpaul et al., 2017;

Zahedi et al., 2022). According to Tabatabaei and Ehsanzadeh (2016), salt stress causes stomata to close, which lowers the concentration of CO_2 accessible for fixation and decreases the activity of CO_2-fixing enzymes. As a result, salinized plants suffer from a significant reduction in gas exchange and disruption of their photosynthetic system, which negatively impacts photosynthesis.

It has been shown that a number of NPs can promote salinity-stressed plant growth and development at concentrations below certain thresholds (Ali et al., 2021; Aslani et al., 2014; Zulfiqar and Ashraf, 2021). By acting as ROS scavengers, nanoparticles can lessen oxidative stress in plant cells and assist in controlling ion distribution and transport once they are inside the plant. Empirical research has demonstrated that some nanoparticles, such as silicon nanoparticles, can improve the uptake of vital nutrients while decreasing the uptake of harmful ions, such as sodium (Abdoli et al., 2020; Gaafar et al., 2020; Gonz§alez-García et al., 2021; Mushtaq et al., 2020).

In this study, salinity caused a significant ($p<0.05$) reduction of the stressed*Zea mays* root by 2.66% and the shoot length by 2.78% (Table 4). However, daily application of a 5 ml iron oxide nanoparticle solution significantly ($p<0.05$) improved the saline-stressed root (sample D) by 9.87% over control. However, no remarkable improvement was noted in the shoot biomass on application of the FeONPs. Considering that the application of FeO-NPs on the unsalinized Zea may (sample C) improved the shoot and root length by 8.97% and 0.99%, respectively, this indicates that the no significant ($p<0.05$) effect observed on the shoot length of the FeONPs-treated salanized *Zea mays* may have resulted from the counter effects of the salinity. However, treatment with bulk $FeCl_3.6H_2O$ improved the root and shoot lengths of the salinized*Zea mays* by 12.51% and 1.82%, respectively (Table 4). Similar treatments showed an improvement of 39.36%, 256.34%, 77.01%, and 175.71% over control in the cases of carotenoid, chlorophyll a, chlorophyll b, and total chlorophyll, respectively. The efficacy of antioxidant enzymes like CAT and SOD was also found to be enhanced by the FeONPs over the control by 13.33% and 80.95%, respectively (Table 4).

The activities of SOD were recorded higher ($p<0.05$) in the positive control (sample B), indicating the induction of stress by the treatment (Fig. 7). This observation corroborates those of Lushchak and Storey (2021) and Sami et al. (2020) who reported that the induction of oxidative stress is usually noted by the upregulation of the activities of antioxidant enzymes like catalase, superoxide dismutase, and peroxidase. Significant activity ($p<0.05$) reduction noted in the FeONPs-treated group comparable to the positive control (Pot B) is indicative of the ameliorative effect of the NPs. In the same vein, in the sample treated with the bulk metal ions, no significant ($p<0.05$) activity was noted when compared to the untreated sample B, indicating that the bulk metal ions could not ameliorate the oxidative stress. Sample C, which was not induced but treated with the nanoparticles, showed no significant ($p<0.05$) activity when compared to sample A, indicating that foliar application of the nanoparticles may not have induced oxidative stress. The significant ($p<0.05$) reduction of the superoxide activities in sample C, comparable to the positive control (B), clearly justified the mitigating role of the nanoparticles in reducing oxidative stress. This finding agrees with Moradbeygi et al. (2020), that an increase in phenolic and flavonoid contents and a decrease in antioxidant enzyme activities occurs in *Dracocephalum moldavica L.* root under saline stress.

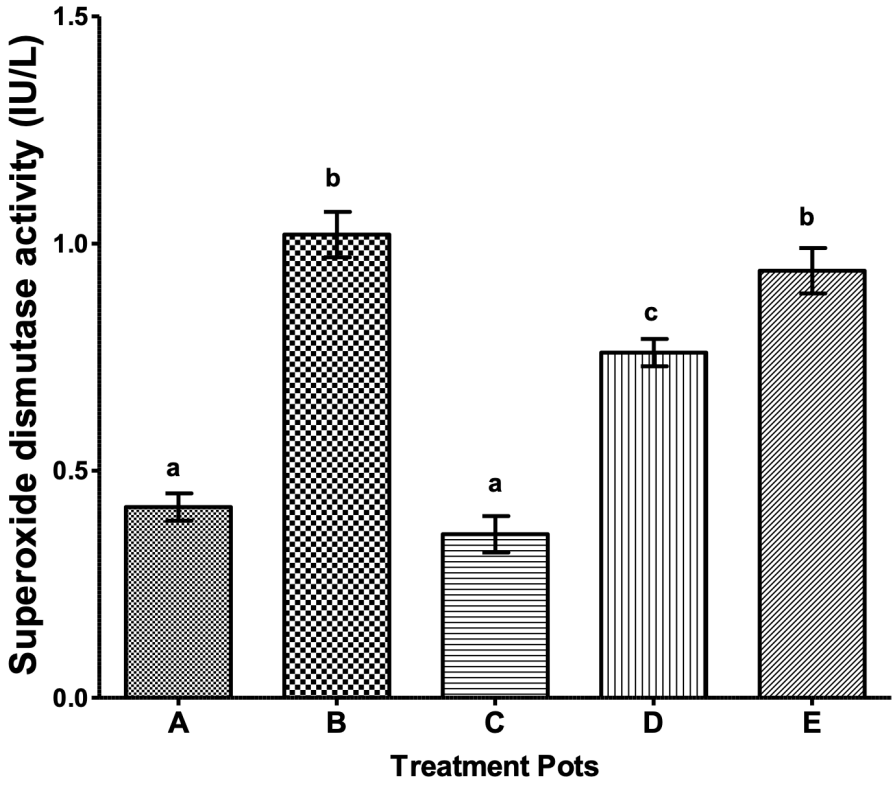

Figure 7. Superoxide dismutase (SOD) activity (IU) of Sodium chloride (NaCl) stressed *Zea mays.* Bars are the mean ± standard deviations of triplicate determinations. Bars bearing different letter(s) are statistically remarkable ($p<0.05$).

The activities of CAT were recorded higher in sample B, indicating the induction of stress by the treatment (Fig. 8). In the sample E treated with the bulk metal ions, no significant ($p<0.05$) activity was noted when compared to the untreated sample B, indicating that the bulk metal ions could not ameliorate the induced oxidative stress. Samples C and D showed no significant ($p<0.05$) activity when compared to sample A, indicating that foliar application of the nanoparticles did not induce further oxidative stress. The significant ($p<0.05$) reduction of the catalase activities in samples C and D when compared to sample B clearly justified the mitigating role of the nanoparticles in oxidative stress reduction (supplementary attachment 1). This finding agrees with Rico et al. (2015), who reported that iron nanoparticles serve a similar role as catalase (CAT) under some circumstances and also aid in neutralizing excess ROS. By moving electrons between various oxidation states, iron is capable of redox cycling. It can engage in redox processes and contribute to the balancing of cellular redox status and the mitigation of oxidative stress because of its capacity to exchange between oxidation states (Koppenol and Hider, 2019).

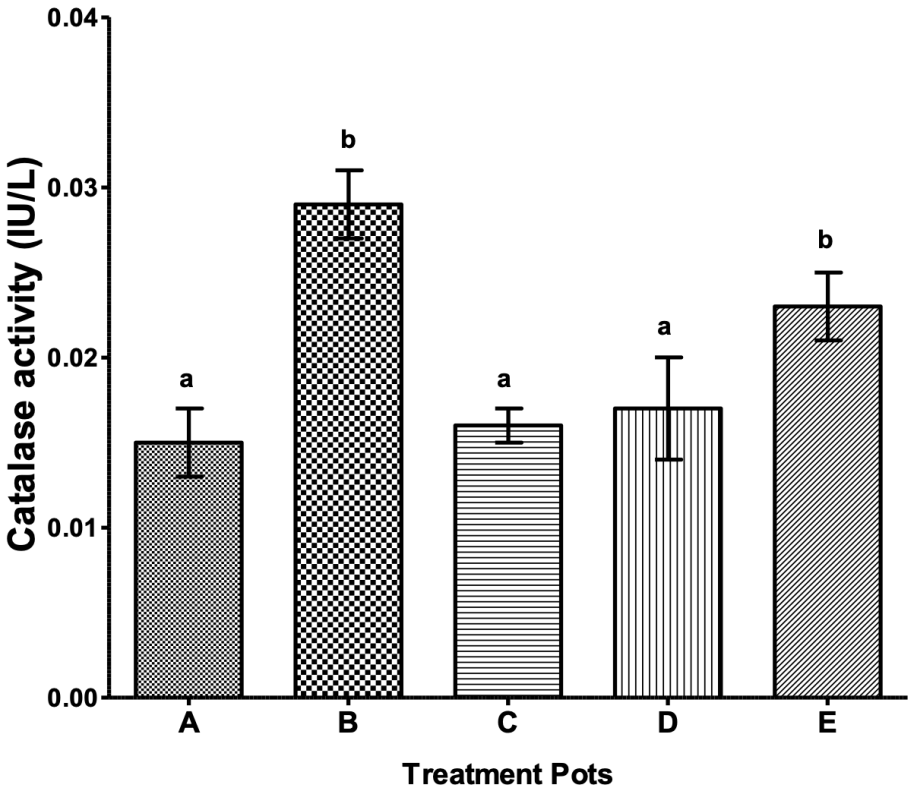

Figure 8. Catalase activity (IU) of Sodium chloride (NaCl) stressed *Zea mays.* Different letter(s) per bar are statistically remarkable ($p<0.05$).

Sustaining photosynthetic efficiency promotes overall plant growth. Nanoparticles are able to stop chlorophyll and other photosynthetic pigments from degrading when exposed to salt stress. All the treatment groups (C, D, and E) showed a tremendous increase ($p > 0.05$) in chlorophyll a and b contents in comparison to the control groups (A and B) (Fig. 9a and Fig. 9b). However, the group treated with the bulk metal showed a significant ($p > 0.05$) reduction in chlorophyll a content when compared to the groups treated with the nanoparticles.

Pot C, which was not polluted but treated with the nanoparticles significantly ($p<0.05$), recorded the highest chlorophyll a and b contents when compared to the other groups. This is an indication that the nanoparticles promoted the content of chlorophyll a and b. The group polluted without treatment (B) showed a notable decrease ($p<0.05$) in total chlorophyll levels in comparison to the treated groups (Fig. 9c). Groups C and D, which were treated with the nanoparticles, recorded a significant ($p<0.05$) increase in total chlorophyll content when compared to the other groups.

These results agree with other related works that NPs applied topically can significantly increase a plant's chlorophyll content and boost the plant's ability to produce more complexes for light harvesting, which increases light absorption and enhances photosynthesis (Ali et al., 2021; Zulfiqar and Ashraf, 2021; Haydar et al. 2022; Alabdallah and Alzahrani, 2020; Gohari et al. 2020b).

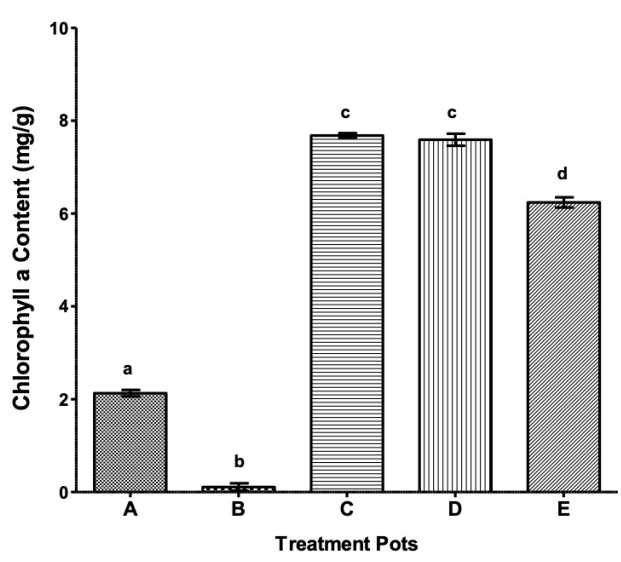

a

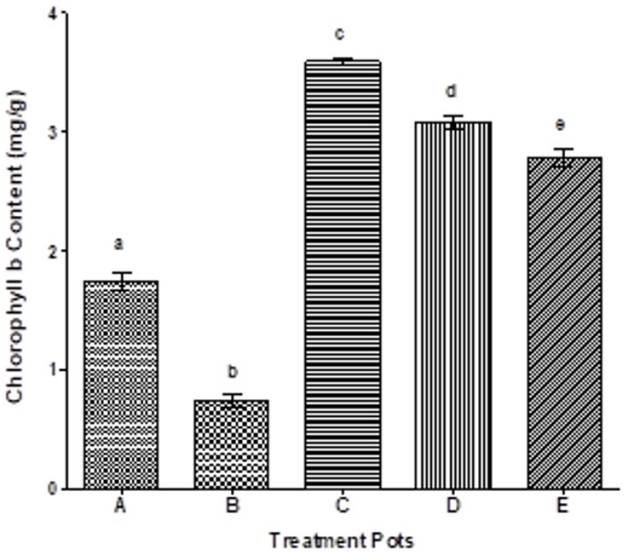

b

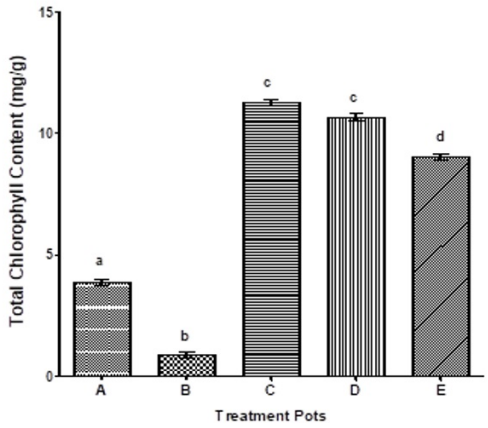

c

Figure 9. a, **b** and **c** represents chlorophyll a and chlorophyll b Contents (mg/g) of sodium chloride (NaCl) stressed *Zea mays*. Different letter(s) per bar are statistically remarkable ($p<0.05$).

Figure 10 shows the carotene content of the saline-stressed*Zea mays*. The group treated with the FeONPs (group D) significantly ($p<0.05$) recorded the highest carotenoid content when compared to the control and the other treatment groups (supplementary attachment 1).

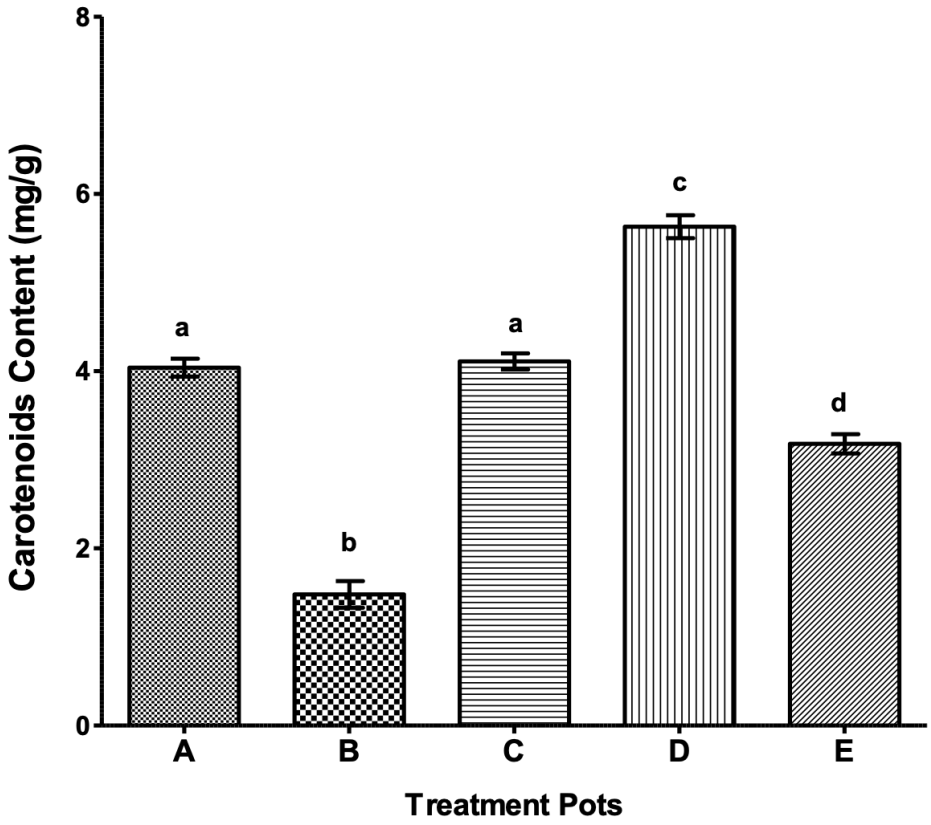

Figure 10. Carotenoids Content (mg/g) of Sodium chloride (NaCl) stressed *Zea mays*. Different letter(s) per bar are statistically remarkable ($p<0.05$).

Salinity negatively affected all the studied indices in the salinized pot B (Table 4). The high activities of the oxidative stress biomarkers catalase and superoxide dismutase recorded in the same pot B is a confirmation of stress. Treatment with iron nanoparticles (sample D) remarkably reversed almost all the observed effects. The significant reduction ($p<0.05$) of CAT and SOD activities compared to the positive control (Pot B) indicates the scavenging role of the NPs. This finding agrees with Ahmed et al., (2023) who reported that foliar application of iron nanoparticles can promote the growth of *Soliddago virgaureal.*

Table 4. Percentage Indices of the samples

POTS	% Indices							
	Root Length	Shoot Length	Caro.	Chloro. A	Chloro. b	Total Chloro	SOD	CAT
B	-2.66	-2.78	-63.37	-94.84	-57.47	-78.04	142.86	93.33
C	0.99	8.97	1.73	260.56	106.32	191.21	-14.29	6.67
D	9.87	-2.71	39.36	256.34	77.01	175.71	80.95	13.33
E	12.56	1.82	-21.29	192.96	59.77	133.07	123.81	53.33

Key: *-ve and +ve signs indicate reduction and increment respectively, comparison to the control*

Conclusion

In this study, FeONPs were synthesized using leaf extract of*Diodella sarmentosa (SW) Bacigalupo El & Cabral ex Borhidi)* at 80 0C. The leaf extract served as reducing agent for the extraction of iron nanoparticles from iron (iii) chloride hexahydrate ($FeCl_3.6H_2O$). The synthesized spherical and amorphous iron nanoparticles with the size ranging from 2.22 to 27.83 nm, were confirmed at the maximum light absorption peak of 380 m to have about 2.5Kev energy. Foliar application of the FeONPs on the saline stressed *Zea mays* ameliorated the adverse effects of salinity on plants by increasing the chlorophyll and carotenoid contents of the plant, and enhancing enzymatic activity of SOD and CAD (antioxidant enzymes). The overall result suggests that iron oxide nanoparticles may be a beneficial agent to enhance plant tolerance to salinity.

Supplementary Material

Supplementary attachment 1

Samples	SOD (IU)	Cata (IU/ml)	Chlo a (mg/g)	Chlo b (mg/g)	T. Chlo (mg/g	Caro (mg/g)
A	0.42 ± 0.03a	0.015 ±0.002a	2.13 ± 0.07a	1.74 ± 0.08a	3.87 ± 0.12a	4.04 ± 0.10a
B	1.02 ± 0.05b	0.029 ±0.002b	0.11 ± 0.08b	0.74 ± 0.05b	0.85 ± 0.14b	1.48 ± 0.15b
C	0.36 ± 0.04a	0.016 ±0.001a	7.68 ± 0.05c	3.59 ± 0.03c	11.27 ± 0.11c	4.11 ± 0.09a
D	0.76± 0.03c	0.017 ±0.003a	7.59 ± 0.13c	3.08 ± 0.06c	10.67 ±0.14c	5.63 ± 0.13c
E	0.94 ± 0.05b	0.023 ±0.002b	6.24 ± 0.11d	2.78 ± 0.07d	9.02 ± 0.13d	3.18 ± 0.11d

Biochemical Analysis of the Plants

Supplementary attachment 2

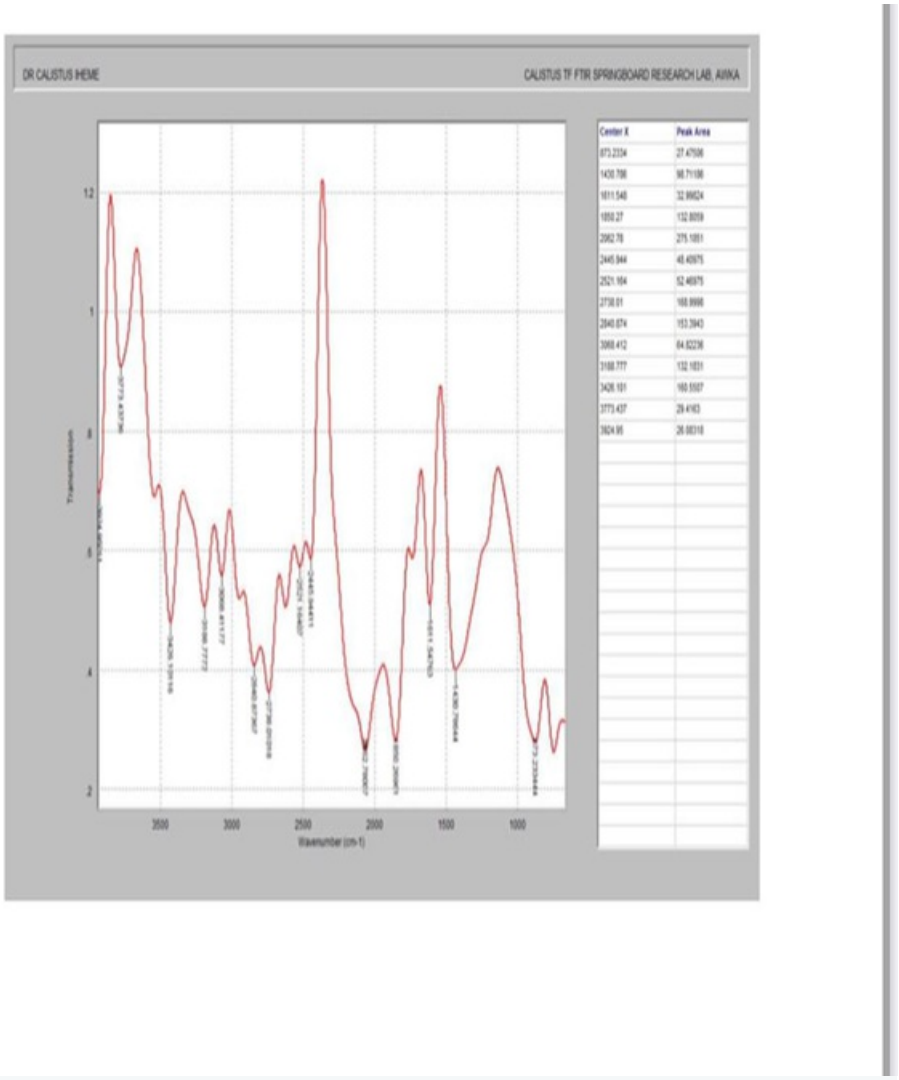

FTIRspectra of the synthesized Fe nanoparticles

Supplementary attachment 3

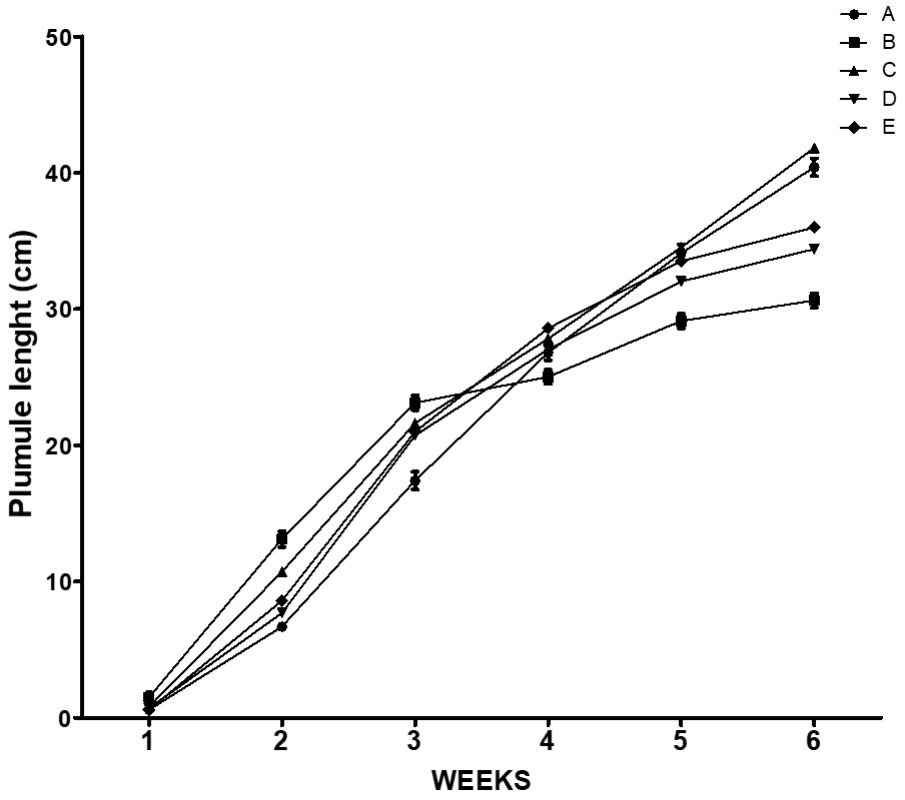

Plumule length

Supplementary attachment 4

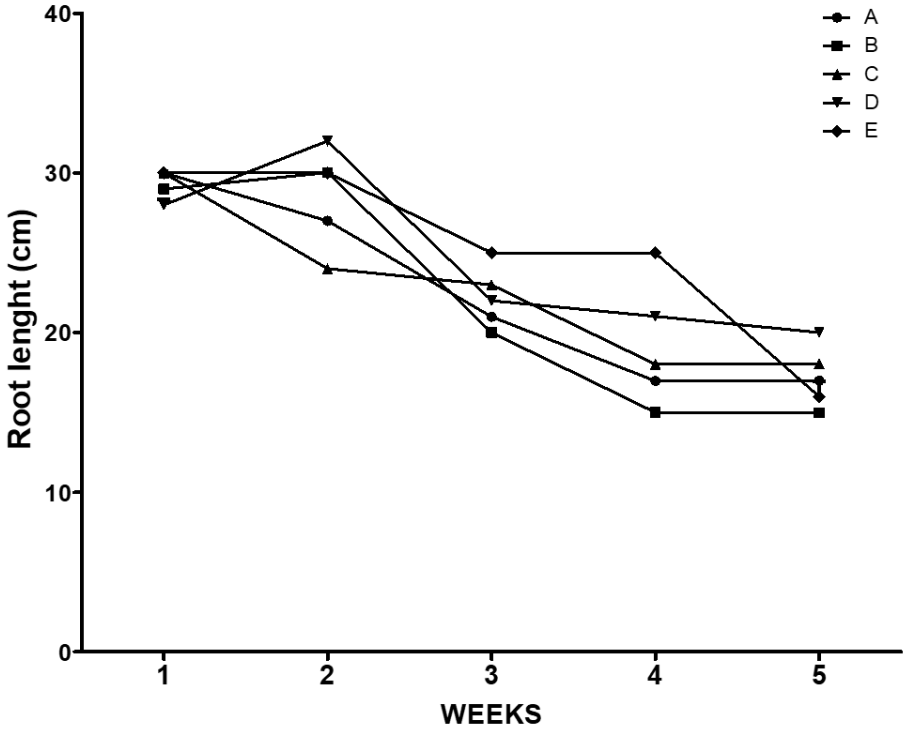

Root length

References

- Abdoli, S., Ghassemi-Golezani, K., and Alizadeh-Salteh, S., (2020). Responses of ajowan (Trachyspermum ammi L.) to exogenous salicylic acid and iron oxide nanoparticles under salt stress. Environ. Sci. Pollut. Res. 27, 36939–36953.
- Achilles, C. N., Morris, R. V., Chipera, S. J., Ming, D. W., & Rampe, E. B. (2013). X-ray diffraction reference intensity ratios of amorphous and poorly crystalline phases: Implications for CheMin on the Mars Science Laboratory Mission. In *Lunar and Planetary Science Conference XLIV*. Houston, TX, Abstract 3072.
- Aebi, H. (1984). Catalase in vitro. *Meth. Enzymol.* 105, 121–126. doi: 10.1016/S0076-6879(84)05016-3
- Ahmad R., Jamil S., Shahzad M., Zorb C., Irshad U., Khan N., Khan S. A. (2017). Metabolic profiling to elucidate genetic elements due to salt stress. CLEAN - Soil, Air, Water, 45 (12), 1600574. doi: 10.1002/clen.201600574.
- Ahmad, I. and Akhtar M.S. (2019). Use of nanoparticles in alleviating salt stress. In: Akhtar M.S., editor. Salt stress, Microbes, and plant interactions: Causes and solution. *Springer, Singapore.* **1**:199-215.
- Ahmed, Mohamed Abdulla; Shafiei-Masouleh, Seyedeh-Somayyeh; Mohsin, Riyadh Mannaa; Salih, Ziyad Khalf (2023). Foliar Application of Iron Oxide Nanoparticles Promotes Growth, Mineral Contents, and Medicinal Qualities of Solidago virgaurea L. Journal of Soil Science and Plant Nutrition. 2610:23(2).
- Alabdallah, M.N. and Alzahrani, H.S. (2020). The potential mitigation effect of ZnO nanoparticles on [*Abelmoschus esculentus* L. Moench] metabolism under salt stress conditions. *Saudi Journal of Biological Sciences*, ***27***(11), 3132-3137.
- Ali, S., Mehmood, A., and Khan, N., (2021). Uptake, translocation, and consequences of nanomaterials on plant growth and stress adaptation. J. Nanomater. 2021, 1–17.
- Álvarez-Chimal, R., & Ángel Arenas-Alatorre, J. (2023). Green synthesis of nanoparticles. A biological approach. IntechOpen. doi: 10.5772/intechopen.1002203.
- Aslani, F., Bagheri, S., Muhd Julkapli, N., Juraimi, A.S., Hashemi, F.S.G., and Baghdadi, A., (2014). Effects of engineered nanomaterials on plants growth: an overview. Sci. World J. 2014, 641759.
- Chaves, M., Flexas, J., and Pinheiro, C., (2009). Photosynthesis under drought and salt: regulation mechanisms from whole plant to cell. Ann Bot. 103(4):551-60. doi: 10.1093/aob/mcn125.
- Etesami, H., and Glick, B.R., (2020). Halotolerant plant growth–promoting bacteria: prospects for alleviating salinity stress in plants. Environ. Exp. Bot. 178, 104124.
- Etesami, H., and Jeong, B.R., (2018). Silicon (Si): review and future prospects on the action mechanisms in alleviating biotic and abiotic stresses in plants. Ecotoxicol. Environ. Saf. 147, 881–896.
- Etesami, H., and Noori, F. (2019). Soil Salinity as a Challenge for Sustainable Agriculture and Bacterial-Mediated Alleviation of Salinity Stress in Crop Plants. In: Kumar, M., Etesami, H., Kumar, V. (eds) Saline Soil-based Agriculture by Halotolerant Microorganisms. Springer, Singapore. https://doi.org/10.1007/978-981-13-8335-9_1
- Etesami, H., Fatemi, H., and Rizwan, M. (2021). Interactions of nanoparticles and salinity stress at physiological, biochemical and molecular levels in plants: A review, Ecotoxicology and Environmental Safety, Volume 225,112769,

ISSN0147-6513, https://doi.org/10.1016/j.ecoenv.2021.112769

- Etesami, H., and Beattie, G.A. (2018). Mining halophytes for plant growth-promoting halotolerant bacteria to enhance the salinity tolerance of non-halophytic crops. Front. Microbiol., 9, p. 148.
- Farooq, M., Hussain, M., Wakeel, A.*et al.* (2015). Salt stress in maize: effects, resistance mechanisms, and management. A review. *Agron. Sustain. Dev.* **35**, 461–481. https://doi.org/10.1007/s13593-015-0287-0
- Feng, Y.; Kreslavski, V.D.; Shmarev, A.N.; Ivanov, A.A.; Zharmukhamedov, S.K.; Kosobryukhov, A.; Yu, M.; Allakhverdiev, S.I.; and Shabala, S. (**2022).** Effects of Iron Oxide Nanoparticles (Fe_3O_4) on Growth, Photosynthesis, Antioxidant Activity and Distribution of Mineral Elements in Wheat (*Triticum aestivum*) Plants. *Plants* **2022**, *11*, 1894. https://doi.org/10.3390/plants11141894
- Fita, A., Rodríguez-Burruezo, A., Boscaiu, M., Prohens, J., Vicente, O., (2015). Breeding and domesticating crops adapted to drought and salinity: a New paradigm for increasing food production. Front. Plant Sci. 6, 978.
- Gaafar, R., Diab, R., Halawa, M., Elshanshory, A., El-Shaer, A., and Hamouda, M., (2020). Role of zinc oxide nanoparticles in ameliorating salt tolerance in soybean. Egypt. J. Bot. 60, 733–747.
- Gohari, G., Safai, F., Panahirad, S., Akbari, A., Rasouli, F., Dadpour, M.R., Fotopoulos, V., (2020b). Modified multiwall carbon nanotubes display either phytotoxic or growth promoting and stress protecting activity in Ocimum basilicum L. in a concentration-dependent manner. Chemosphere 249, 126171.
- Gonz´alez-García, Y., C´ardenas-´Alvarez, C., Cadenas-Pliego, G., Benavides-Mendoza, A., Cabrera-de-la-Fuente, M., Sandoval-Rangel, A., Vald´es-Reyna, J., and Ju´arez-Maldonado, A., (2021). Effect of three nanoparticles (Se, Si and Cu) on the bioactive compounds of bell pepper fruits under saline stress. Plants 10, 217.
- Haydar MS, Ghosh S, Mandal P (2022) Application of iron oxide nanoparticles as micronutrient fertilizer in mulberry propagation. J Plant Growth Regul. 41:1726–1746.
- Iqbal, M.S., Singh, A.K., Singh, S.P and Ansari, M.I. (2020). Nanoparticles and plant interaction with respect to stress response nanomaterials and environmental Biotechnology. *Springer*, **1**: 1-15.
- Isayenkov SV, Maathuis FJM. 2019. Plant salinity stress: many unanswered questions remain. Frontiers in Plant Science 10: 80.
- Kaleem, Fawad & Shabir, Ghulam & Aslam, Kashif & Rasul, Sumaira & Manzoor, Hamid & Masood, Shahid & Khan, Abdul Rehman. (2018). An Overview of the Genetics of Plant Response to Salt Stress: Present Status and the Way Forward. Applied Biochemistry and Biotechnology. 186. 10.1007/s12010-018-2738-y.
- Khan A., Anwar Y., Hasan M., Iqbal A., Ali M., Alharby H., et al.. (2017). Attenuation of drought stress in Brassica seedlings with exogenous application of Ca2+ and H2O2. Plan. Theory 6:20.10.3390/plants602002.
- Komaresofla, B.R., Alikhani, H.A. Etesami, H. and Khoshkholgh-Sima, N.A. (2019). Improved growth and salinity tolerance of the halophyte Salicornia sp. by co–inoculation with endophytic and rhizosphere bacteria. Appl. Soil Ecol., 138, pp. 160-170.
- Koppenol, W.H. and R.H. Hider, (2019). Iron and redox cycling. Do's and don'ts, Free Radical Biology and Medicine, Volume 133, 2019, Pages 3-10.
- Kumar, B. (**2021**). Green Synthesis of Gold, Silver, and Iron Nanoparticles for the Degradation of Organic Pollutants in Wastewater. *J. Compos. Sci.* **2021**, *5*, 219. https://doi.org/10.3390/jcs5080219

- Liang, W., Ma, X., Wan, P., and Liu, L., (2018). Plant salt-tolerance mechanism: a review. Biochem. Biophys. Res. Commun. 495, 286–291.
- Lushchak VI, and Storey KB (2021). Oxidative stress concept updated: Definitions, classifications, and regulatory pathways implicated. EXCLI J. 2021 May 26;20:956-967. doi: 10.17179/excli2021-3596. PMID: 34267608; PMCID: PMC8278216.
- Maria, G., Zoltán, K., Viktória K.K. et al., (2022). Iron nanoparticles for plant nutrition: Synthesis, transformation, and utilization by the roots of Cucumis sativus. *Journal of Materials Research,* **38**: 1035–1047.
- Martin Stpaul, N., Delzon, S., and Cochard, H., (2017). Plant resistance to drought depends on timely stomatal closure. Ecol. Lett. 20, 1437e1447.
- Mattiello, A., Filippi, A., Po˘s´ci´c, F., Musetti, R., Salvatici, M.C., Giordano, C., Vischi, M., Bertolini, A., and Marchiol, L., (2015). Evidence of phytotoxicity and genotoxicity in Hordeum vulgare L. exposed to CeO2 and TiO2 nanoparticles. Front. Plant Sci. 6, 1043.
- Mauricio, M.D., Guerra-Ojeda, S., Marchio, P., Valles, S.L., Aldasoro, M., Escribano-Lopez, I., Herance, J.R., Rocha, M., Vila, M.J. and Victor, V.M. (2018). Nanoparticles in medicine: A focus on vascular oxidative stress *Oxidative Medicine and Cellular Longevity,* 1-20.
- Mittal S., Kumari N., and Sharma V. (2011). Differential responses of seven contrasting species to high light using pigments and chlorophyll a fluorescence. J. Stress Physiol. Biochem. 7(2), 20-33.
- Moradbeygi, H., Jamei, R., Heidari, R., and Darvishzadeh, R., (2020). Investigating the enzymatic and non-enzymatic antioxidant defense by applying iron oxide nanoparticles in Dracocephalum moldavica L. plant under salinity stress. Sci. Hortic. 272, 109537.
- Mukherjee, S.P. and Choudhuri, M.A. (1983) Implication of Water Stress—Induced Changes in the Levels of Endogenous Ascorbic Acid and Hydrogen Peroxide in Vigna Seedling. Physiologia Plantarum, 58, 166-170. http://dx.doi.org/10.1111/j.1399-3054.1983.tb04162.x
- Mushtaq, A., Khan, Z., Khan, S., Rizwan, S., Jabeen, U., Bashir, F., Ismail, T., Anjum, S., and Masood, A., (2020). Effect of silicon on antioxidant enzymes of wheat (Triticum aestivum L.) grown under salt stress. Silicon 12, 2783–2788.
- Nair, R., Varghese, S.H., Nair, B.G., Maekawa, T., Yoshida, Y., Kumar, D.S., 2010. Nanoparticulate material delivery to plants. Plant Sci. 179, 154–163.
- Paramo, L.A., Feregrino-P´erez, A.A., Guevara, R., Mendoza, S., and Esquivel, K., (2020). Nanoparticles in agroindustry: applications, toxicity, challenges, and trends. Nanomaterials 10, 1654.
- Rico, C.M., Peralta-Videa, J.R., and Gardea-Torresdey, J.L., (2015). Chemistry, biochemistry of nanoparticles, and their role in antioxidant defense system in plants. In: Siddiqui, M., Al-Whaibi, M., Mohammad, F. (Eds.), Nanotechnology and Plant Sciences. Springer, Cham. https://doi.org/10.1007/978-3-319-14502-0_1.
- Rout and Sahoo (2015). Reviews in Agricultural Science, 3:1-24, 2015. doi: 10.7831/ras.3.1
- Sami, F., Siddiqui, H., and Hayat, S., (2020). Impact of silver nanoparticles on plant physiology: a critical review. In: Hayat, S., Pichtel, J., Faizan, M., Fariduddin, Q. (Eds.), Sustainable Agriculture Reviews 41. Sustainable Agriculture Reviews, vol 41. Springer, Cham. https://doi.org/10.1007/978-3-030-33996-8_6.

- Shah, Muhammad & Guan, Zheng-Hui & Khan, Alauddin & Ali, Amjad & Rehman, Ata & Faisal, Shah & Saud, Shah & Adnan, Muhammad & Wahid, Fazli & Alamri, Saud & Siddiqui, Manzer & Ali, Shamsher & Jatoi, Wajid & Hammad, Hafiz & Fahad, Shah. (2021). Synthesis of silver nanoparticles using Plantago lanceolata extract and assessing their antibacterial and antioxidant activities. Scientific Reports. 11. 20754. 10.1038/s41598-021-00296-5.
- Singh, A.; Sengar, R.S.; Shahi, U.P.; Rajput, V.D.; Minkina, T.; and Ghazaryan, K.A. (2023). Prominent Effects of Zinc Oxide Nanoparticles on Roots of Rice (Oryza sativa L.) Grown under Salinity Stress. Stresses, 3, 33–46. https://doi.org/10.3390/stresses3010004
- Šutka, A., Vanags, M., Spule A. et al. (2020). Identifying iron-bearings nanoparticles precursor for thermal transformation into the highly active hematite photo-fenton catalyst. *Catalyst.* **10**: 778.
- Tabatabaei, S., and Ehsanzadeh, P., (2016). Photosynthetic pigments, ionic and antioxidative behaviour of hulled tetraploid wheat in response to NaCl. Photosynthetica 54, 340e350.
- Tharani K. & Nehru L.C. (2015). Synthesis and Characterization of Iron Oxide Nanoparticle by Precipitation Method International Journal of Advanced Research in Physical Science (IJARPS) Volume 2, Issue 8, August 2015, PP 47-50 ISSN 2349-7874 (Print) & ISSN 2349-7882 (Online).
- Tripathi, D.K., Shweta, Singh, S., Singh, S., Pandey, R., Singh, V.P., Sharma, N.C., Prasad, S.M., Dubey, N.K., and Chauhan, D.K., (2017a). An overview on manufactured nanoparticles in plants: Uptake, translocation, accumulation and phytotoxicity. Plant Physiol. Biochem. 110, 2–12.
- United Nations. (2019). World Population Prospects: The 2019 Revision. New York: United Nations.
- Van Zelm, E., Zhang, Y., and Testerink, C., (2020). Salt tolerance mechanisms of plants. Annu Rev Plant Biol.: 71:403-433. doi: 10.1146/annurev-arplant-050718-100005.
- Zahedi, S.M., Hosseini, M.S., Naghmeh, D., Abadía, J., Germ, M., Gholami, R., and Abdelrahman, M., (2022). Evaluation of drought tolerance in three commercial pomegranate cultivars using photosynthetic pigments, yield parameters and biochemical traits as biomarkers. Agric. Water Manag. 261, 107357.
- Zhang, H., Chen, F., Wang, X., and Yao, H. (2006). Evaluation of antioxidant activity of parsley (Petroselinum crispum) essential oil and identification of its antioxidant constituents, Food Research International, Volume 39, Issue 8, 2006, Pages 833-839, ISSN 0963-9969, https://doi.org/10.1016/j.foodres.2006.03.007.
- Zörb, C., Geilfus, C. M., & Dietz, K. J. (2019). Salinity and crop yield. In*Plant Biology* (Vol. 21, pp. 31–38). Blackwell Publishing Ltd. https://doi.org/10.1111/plb.12884.
- Zulfiqar, F., Ashraf, M., (2021). Nanoparticles potentially mediate salt stress tolerance in plants. Plant Physiol. Biochem. 160, 257–268.
- Isayenkov SV, and Maathuis FJM. (2019). Plant salinity stress: many unanswered questions remain. Frontiers in Plant Science 10: 80.